BIOCHEMISTRY
including biophysical chemistry & molecular biology

Article

pubs.acs.org/biochemistry

Distinct Disulfide Isomers of μ-Conotoxins KIIIA and KIIIB Block Voltage-Gated Sodium Channels

Keith K. Khoo,[†,‡,§] Kallol Gupta,[∥] Brad R. Green,[†] Min-Min Zhang,[⊥] Maren Watkins,[⊥] Baldomero M. Olivera,[⊥] Padmanabhan Balaram,[∥] Doju Yoshikami,[⊥] Grzegorz Bulaj,[@] and Raymond S. Norton*[,†]

[†]Medicinal Chemistry, Monash Institute of Pharmaceutical Sciences, Monash University, 381 Royal Parade, Parkville, VIC 3052, Australia

[‡]The Walter & Eliza Hall Institute of Medical Research, 1G Royal Parade, Parkville, VIC 3052, Australia

[§]The Department of Medical Biology, The University of Melbourne, Parkville, Victoria 3010, Australia

[∥]Molecular Biophysics Unit, Indian Institute of Science, Bangalore 560 012, India

[⊥]Department of Biology, University of Utah, Salt Lake City, Utah 84112, United States

[@]Department of Medicinal Chemistry, College of Pharmacy, University of Utah, Salt Lake City, Utah 84108, United States

Supporting Information

ABSTRACT: In the preparation of synthetic conotoxins containing multiple disulfide bonds, oxidative folding can produce numerous permutations of disulfide bond connectivities. Establishing the native disulfide connectivities thus presents a significant challenge when the venom-derived peptide is not available, as is increasingly the case when conotoxins are identified from cDNA sequences. Here, we investigate the disulfide connectivity of μ-conotoxin KIIIA, which was predicted originally to have a [C1−C9,C2−C15,C4−C16] disulfide pattern based on homology with closely related μ-conotoxins. The two major isomers of synthetic μ-KIIIA formed during oxidative folding were purified and their disulfide connectivities mapped by direct mass spectrometric collision-induced dissociation fragmentation of the disulfide-bonded polypeptides. Our results show that the major oxidative folding product adopts a [C1−C15,C2−C9,C4−C16] disulfide connectivity, while the minor product adopts a [C1−C16,C2−C9,C4−C15] connectivity. Both of these peptides were potent blockers of $Na_V1.2$ (K_d values of 5 and 230 nM, respectively). The solution structure for μ-KIIIA based on nuclear magnetic resonance data was recalculated with the [C1−C15,C2−C9,C4−C16] disulfide pattern; its structure was very similar to the μ-KIIIA structure calculated with the incorrect [C1−C9,C2−C15,C4−C16] disulfide pattern, with an α-helix spanning residues 7−12. In addition, the major folding isomers of μ-KIIIB, an N-terminally extended isoform of μ-KIIIA identified from its cDNA sequence, were isolated. These folding products had the same disulfide connectivities as μ-KIIIA, and both blocked $Na_V1.2$ (K_d values of 470 and 26 nM, respectively). Our results establish that the preferred disulfide pattern of synthetic μ-KIIIA and μ-KIIIB folded in vitro is 1−5/2−4/3−6 but that other disulfide isomers are also potent sodium channel blockers. These findings raise questions about the disulfide pattern(s) of μ-KIIIA in the venom of *Conus kinoshitai*; indeed, the presence of multiple disulfide isomers in the venom could provide a means of further expanding the snail's repertoire of active peptides.

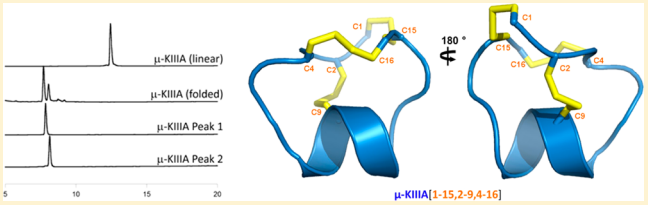

Disulfide bonds are a common feature of peptides and proteins that function outside the cell and are generally regarded as being essential for both the stability and the maintenance of the native structure.[1,2] There is evidence, however, that they can be reduced and scrambled in vivo by agents such as glutathione, serum albumin, or redox enzymes,[3−5] with possible losses of native structure and biological activity. Several strategies have been implemented to replace disulfide bridges with more stable linkages, including diselenides,[6,7] thioethers such as lanthionine, in which one of the sulfur atoms of the disulfide bond is eliminated,[8] cystathionine, in which one of the sulfur atoms is replaced with a methylene group,[9,10] or dicarba bridges, in which the disulfide is replaced with a carbon−carbon bridge.[11−13]

In peptides with multiple disulfide bonds, establishing the native disulfide connectivities can be challenging. Disulfide mapping methods have generally relied on selective reduction and alkylation of bonded thiol pairs, followed by sequencing using traditional Edman sequencing methods or mass spectrometry.[14−16] This approach is limited by difficulties of selective reduction in the case of multiple disulfide-bonded peptides.[17] Conventional two-dimensional ^1H nuclear magnetic resonance (NMR) spectroscopy can also identify these

Received: September 14, 2012
Revised: November 19, 2012
Published: November 20, 2012

dx.doi.org/10.1021/bi301256s | *Biochemistry* 2012, 51, 9826−9835

connectivities in principle,[16] but spectral overlap of resonances from multiple Cys spin systems often makes it difficult or impossible to decipher the native connectivities in peptides with multiple disulfide bonds.[18,19] As such, alternative NMR-based strategies have been introduced to overcome this problem.[20,21]

Recently, an alternative approach was proposed by Poppe et al.[17] in which the disulfide connectivity was obtained by applying Bayesian rules of inference to the local topology of cysteine residues. This method was then applied to experimental NMR data for three exemplar peptides with complex disulfide connectivities: hepcidin, kalata-B1, and μ-conotoxin KIIIA. In the case of μ-KIIIA, the inferred [C1−C15,C2−C9,C4−C16] connectivity differed from the previously described pattern for this conotoxin, [C1−C9,C2−C15,C4−C16].[22] The [C1−C9,C2−C15,C4−C16] pattern was consistent with the original NMR data set although not uniquely defined by it (for the reasons mentioned above), and the choice of that pattern was dictated predominantly by the ample precedent in the literature for the 1−4/2−5/3−6 disulfide pattern in numerous other μ-conotoxins.[21,23−27] It was further supported by the observation that two-disulfide analogues of μ-KIIIA containing just the [C2−C15] and [C4−C16] bridges showed structures and activity profiles similar to those of μ-KIIIA itself.[22,28,29]

In this paper, we have examined the two major isomers of synthetic μ-KIIIA (named μ-KIIIA-P1 and μ-KIIIA-P2) formed during oxidative folding. Their disulfide connectivities have been mapped by a newly developed mass spectrometry (MS) procedure that is based on the interpretation of the product ions produced upon direct gas-phase fragmentation of the native, disulfide-bonded intact peptides.[15,30] NMR spectra of both the folding isoforms have also been analyzed. The results show that the more abundant product from oxidative folding has the [C1−C15,C2−C9,C4−C16] disulfide pattern observed by Poppe et al.[17] while the minor product has a [C1−C16,C2−C9,C4−C15] pattern. Remarkably, both isomers exhibited blockade of sodium channels, raising questions about which, if either, is the "native" disulfide pattern in the venom of *Conus kinoshitai*, the *Conus* species from which the cDNA sequence encoding this peptide was first isolated.[31] Upon further examination of the cDNA sequence of μ-KIIIA, it was determined that the mature peptide sequence of μ-KIIIA produced in the venom of *C. kinoshitai* possesses two additional residues preceding the N-terminus (Asn1 and Gly2). The N-terminally extended isoform of μ-KIIIA is named μ-KIIIB. The major oxidative isomers of this analogue (μ-KIIIB-P1 and μ-KIIIB-P2) have also been synthesized and their disulfide connectivities and sodium channel blocking activities compared with those of μ-KIIIA.

MATERIALS AND METHODS

Cloning of μ-KIIIB. μ-KIIIB was identified from a cDNA library prepared as described previously.[32] Briefly, a cDNA library was created from the venom duct of an individual *C. kinoshitai* specimen. Total RNA was isolated from the venom duct with TRIzol reagent (TRIzol Total RNA Isolation, Life Technologies/Gibco BRL, Grand Island, NY), and cDNA was prepared using the SMART PCR cDNA Synthesis Kit (Clontech Laboratories, Palo Alto, CA). The cDNA was cloned into the pNEB206A vector (New England BioLabs, Inc., Beverly, MA), and sequences of individual clones were determined by standard automated sequencing.

Synthesis and Oxidative Folding. Peptides were synthesized on a 30 μmol scale on preloaded Fmoc-Cys(Trt)-Rink Amide-MBHA resin (substitution of 0.32 mmol/g) using standard *N*-(9-fluorenyl)methoxycarbonyl (Fmoc) chemistry. The peptides were cleaved from the resin by a 3−4 h treatment with reagent K [82.5/5/2.5/5/5 (by volume) TFA/water/ethanedithiol/phenol/thioanisole mixture]. The cleaved peptides were filtered, precipitated with cold methyl *tert*-butyl ether (MTBE), and washed several times with cold MTBE. The reduced peptides were purified by reversed-phase high-performance liquid chromatography (HPLC) using a semipreparative C18 Vydac column (218TP510, 250 mm × 10 mm, 5 μm particle size) and eluted with a linear gradient from 5 to 35% solvent B over 35 min, where solvent A was 0.1% (v/v) TFA in water and solvent B was 0.1% (v/v) TFA in 90% aqueous acetonitrile. The flow rate was 4 mL/min, and the absorbance was monitored at 220 nm. Purified peptides were quantified by UV absorbance at 280 nm.

Oxidative folding of synthetic μ-KIIIA was accomplished via 2 h glutathione-assisted folding at room temperature under the following conditions: 20 μM linear peptide, 0.1 M Tris-HCl (pH 7.5), 1 mM EDTA, and 1 mM reduced and 1 mM oxidized glutathione. Folding was quenched by acidification via addition of 8% (v/v) formic acid. Folded peptides were purified by reversed-phase HPLC using a semipreparative C18 column (218TP510, 250 mm × 10 mm) over a linear gradient ranging from 5 to 35% solvent B over 35 min. Purities of the folded peptides were assessed by analytical HPLC using a linear gradient from 10 to 40% solvent B over 30 min. Quantities of the minor folding product were obtained by repurification using an analytical C18 column (218TP54, 250 mm × 4.6 mm, 5 μm particle size) using identical HPLC conditions. Amounts of the peptide were quantified by UV absorbance at 280 nm. Purified peptides were finally dried by lyophilization, and peptide masses were confirmed by matrix-assisted laser desorption ionization time-of-flight (MALDI-ToF) mass spectrometry.

Mass Spectrometry. The mass spectrometric experiments were performed on an HCT Ultra ETDII ion trap mass spectrometer (Bruker Daltonics, Bremen, Germany). All experiments were performed through liquid chromatography−mass spectrometry (LC−MS) analysis of the samples by coupling the ion trap mass spectrometer with an Agilent 1100 HPLC system. The peptide samples were subjected to LC−MS using a reversed-phase C18 analytical column, with a H_2O/acetonitrile mixture (with 0.1% formic acid) as the solvent system, at a flow rate of 0.2 mL/min. The CID experiment was performed by selecting the precursor ion and subsequently fragmenting it through collision with He gas. The fragmentation amplitude (V_{p-p}) was kept between 1 and 3. The spectra were averaged over four scans.

NMR Spectroscopy. NMR spectra were recorded for μ-KIIIA-P1 (86 μM) and μ-KIIIA-P2 (43 μM) in a 95% H_2O/5% ^2H_2O mixture at pH 4.8 and 5 °C on a Bruker DRX-600 spectrometer. Spectra were processed using TOPSPIN (version 1.3, Bruker Biospin). Spectra recorded as described by Khoo et al.[22] were analyzed using XEASY (version 1.3.13).[33]

Structure Calculations. Structure calculations were run using the original nuclear Overhauser effect (NOE) and dihedral restraint list as described by Khoo et al.[22] (BioMagResBank entry 20048) but with the [C1−C15,C2−C9,C4−C16] disulfide connectivities. Additional structural calculations were run with six additional NOE distance restraints that were consistent with the [C1−C15,C2−

C9,C4−C16] disulfide connectivity but could not be unambiguously determined previously because of peak overlap. Structures were recalculated in XPLOR-NIH[34] using the simulated annealing script. Lowest-energy structures were subjected to energy minimization in water. Final families of the 20 lowest-energy structures were chosen for analysis using PROCHECK-NMR[35] and MOLMOL.[36] Final structures had no experimental distance violations greater than 0.2 Å or dihedral angle violations greater than 5°. Structural figures were prepared using MOLMOL[36] and PyMOL.[53] Final structures have been deposited in the Protein Data Bank as entry 2LXG.

Electrophysiology of the Rat Clones of $Na_V1.2$, 1.4 and 1.7 Expressed in *Xenopus* Oocytes. Oocytes expressing $Na_V1.2$, 1.4 and 1.7 α-subunits were prepared and two-electrode voltage clamped essentially as described previously.[37] Briefly, oocytes were placed in a 30 μL chamber containing ND96 and two-electrode voltage clamped at a holding potential of −80 mV. To activate VGSCs, the membrane potential was stepped to −10 mV for a 50 ms period every 20 s. To apply toxin, the perfusion was halted, 3 μL of the toxin solution (at 10 times the final concentration) was applied to the 30 μL bath, and the bath was manually stirred for ∼5 s by gently aspirating and expelling a few microliters of the bath fluid several times with a pipettor. Toxin exposures were in static baths to conserve material. On rate constants were obtained assuming the equation $k_{obs} = k_{on}[peptide] + k_{off}$,[38] where k_{obs} was determined from the single-exponential fit of the time course of block by a fixed peptide concentration of 10 μM and k_{off} estimated from the level of recovery from block 20 min following toxin washout and assuming recovery followed a single-exponential time course; this procedure for determining k_{off} was adopted because recovery from block was too slow to measure by single-exponential fits.[37] All recordings were taken at room temperature (∼21 °C).

RESULTS

Cloning of μ-KIIIB. The amino acid sequence of μ-KIIIB was deduced from cDNA derived from venom ducts of *C. kinoshitai*, as described previously.[32] μ-KIIIB shared an identical amino acid sequence with μ-KIIIA but included two additional residues at the N-terminus (Asn-Gly).

Synthesis and Oxidative Folding. μ-KIIIA and μ-KIIIB were synthesized chemically using the Fmoc protocols described previously.[31] After oxidation of the synthetic linear peptides, two distinct HPLC peaks for both μ-KIIIA and μ-KIIIB were obtained that yielded identical mass values (1882.6 Da for μ-KIIIA and 2055.4 Da for μ-KIIIB), corresponding to the respective native sequences with three disulfide bonds. Representative reversed-phase HPLC chromatograms of the oxidative folding of μ-KIIIA and μ-KIIIB are shown in Figure 1. The major isomer (μ-KIIIA-P1) elutes earlier than the minor isomer (μ-KIIIA-P2) for μ-KIIIA, while the major isomer (μ-KIIIB-P2) elutes later than the minor isomer (μ-KIIIB-P1) for μ-KIIIB.

Mass Spectrometric Determination of Disulfide Connectivities. Two distinct HPLC peaks of μ-KIIIA, obtained through the oxidation of the synthetic linear peptide, yielded identical mass values (1882.6 Da) corresponding to the native sequence with three disulfide bonds. In principle, 15 disulfide foldamers corresponding to distinct disulfide linkage patterns are possible (Figure S1 of the Supporting Information). Direct MS fragmentation of intact disulfide-bonded

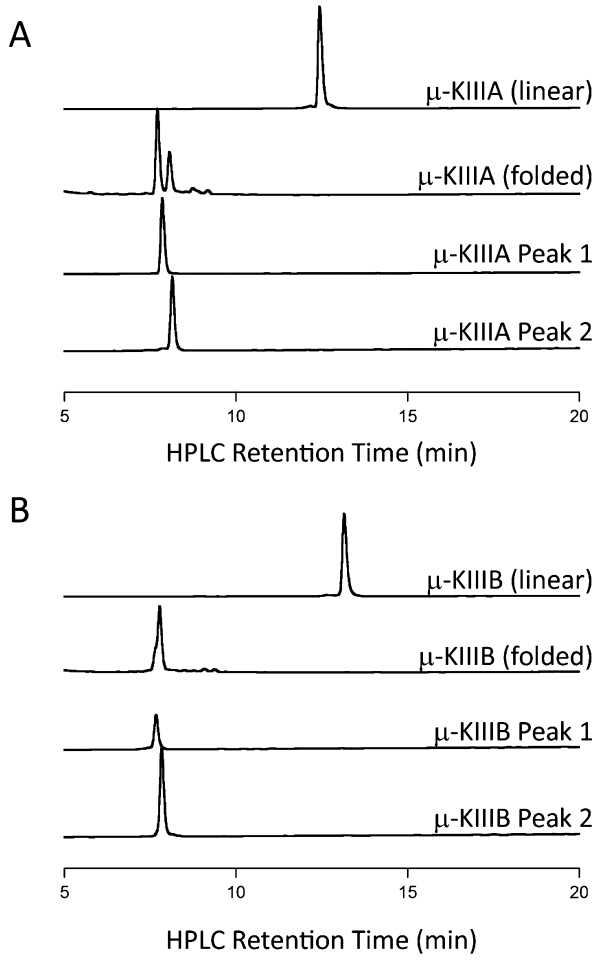

Figure 1. Representative reversed-phase HPLC chromatograms of the oxidative folding of (A) μ-KIIIA and (B) μ-KIIIB. μ-KIIIA peaks 1 and 2 represent the [C1−C15,C2−C9,C4−C16] and [C1−C16,C2−C9,C4−C15] connectivities, respectively (see the text). Folding was conducted in a buffered solution (pH 7.5) containing a mixture of 1 mM oxidized and 1 mM reduced glutathione for 2 h at room temperature.

peptides or proteolyticaly nicked peptides provides a route to de novo determination of disulfide connectivity in natural and synthetic peptides. This procedure relies on the interpretation of different modes of disulfide bond cleavage under ion trap mass spectrometric conditions. The structures of the ions are determined through a program, *DisConnect*, developed to analyze the CID MS/MS data of the native disulfide-bonded molecule. The key steps in establishing disulfide connectivity for the two μ-KIIIA and μ-KIIIB isomers (P1 and P2) are described below.

μ-KIIIA-P1. Upon trypsin digestion, the fraction shows a mass of 1423.6 Da (inset of Figure 2) that corresponds to a peptide in which the central tetrapeptide segment (DHSR) has been excised out by trypsin cleavage at the R−D and R−C15 peptide bonds. In addition, a proteolytic cleavage at the K−W bond is also observed. This means that the tryptic peptide consists of three individual peptide chains that are held together by three disulfide bonds. Foldamers F1, F4, and F7 (Figure S1 of the Supporting Information) cannot yield the observed tryptic peptide. In these cases, because of the C15−C16 connectivity, Arg14 is not inside a disulfide loop and thus would cause separation of the C15−C16 disulfide from the rest of the

dx.doi.org/10.1021/bi301256s | *Biochemistry* 2012, 51, 9826−9835

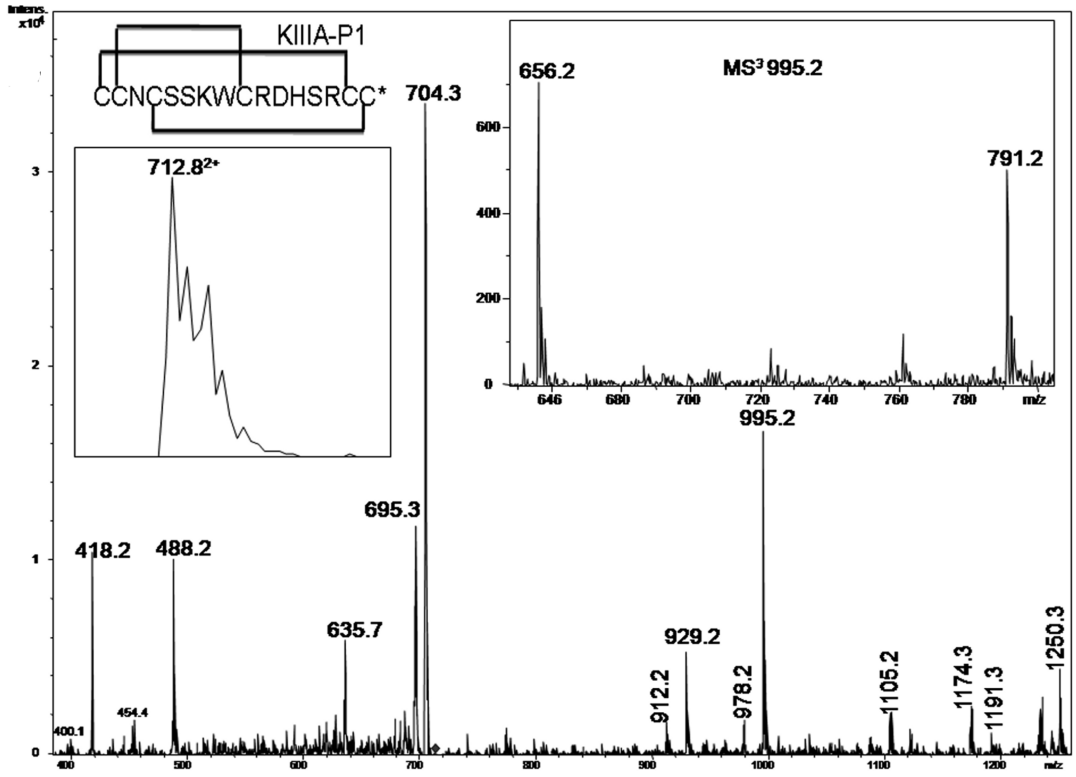

Figure 2. CID MS^2 spectrum of the peptide derived upon trypsin digestion of μ-KIIIA-P1 [m/z 712.8, $(M + 2H)^{2+}$]. The inset shows the MS spectrum of the precursor ion and MS^3 spectra of the ion at m/z 995.2.

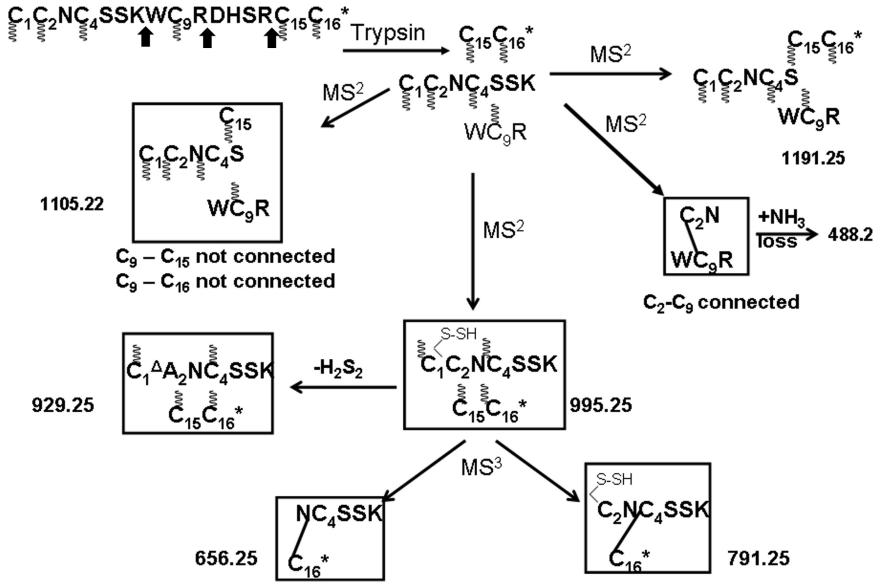

Figure 3. Assignments of the key MS^n fragment ions of tryptic μ-KIIIA-P1. The m/z values of each of the ions are indicated against the respective structures, and they correspond to the singly charged values, unless otherwise specified. For every structure, Cys residues with indeterminate connectivity are indicated with the wavy lines. Subsequently, in the structures from which a particular Cys connectivity is evident, the connected Cys residues are joined through a dashed line. The arrows indicate the site of proteolysis. The 2–4 connectivity is established by the product ion at m/z 488.2, while the ions at m/z 656.2 and 791.2 confirm the 3–6 connectivity.

peptide. Hence, 12 possible foldamers (Figure S2 of the Supporting Information) need to be considered. Figure 2 shows the CID MS/MS spectra of the tryptic peptide. The structures of the major fragment ions are determined through *DisConnect*. The chemical structures of the key ions, derived through the fragmentation of the disulfide-bonded molecule, are shown in Figure 3. The structures shown correspond uniquely to the observed m/z values. A key ion is observed at m/z 488.2 that arises through the loss of NH_3 from an initial product ion, which necessarily must have C2 disulfide bonded to C9. This leaves only two probable foldamers, F11 and F14, to be considered further. A final distinction between these two foldamers is achieved by a subsequent MS^3 fragmentation of the ion at m/z 995.2 (inset of Figure 2). The probable

dx.doi.org/10.1021/bi301256s | *Biochemistry* 2012, 51, 9826–9835

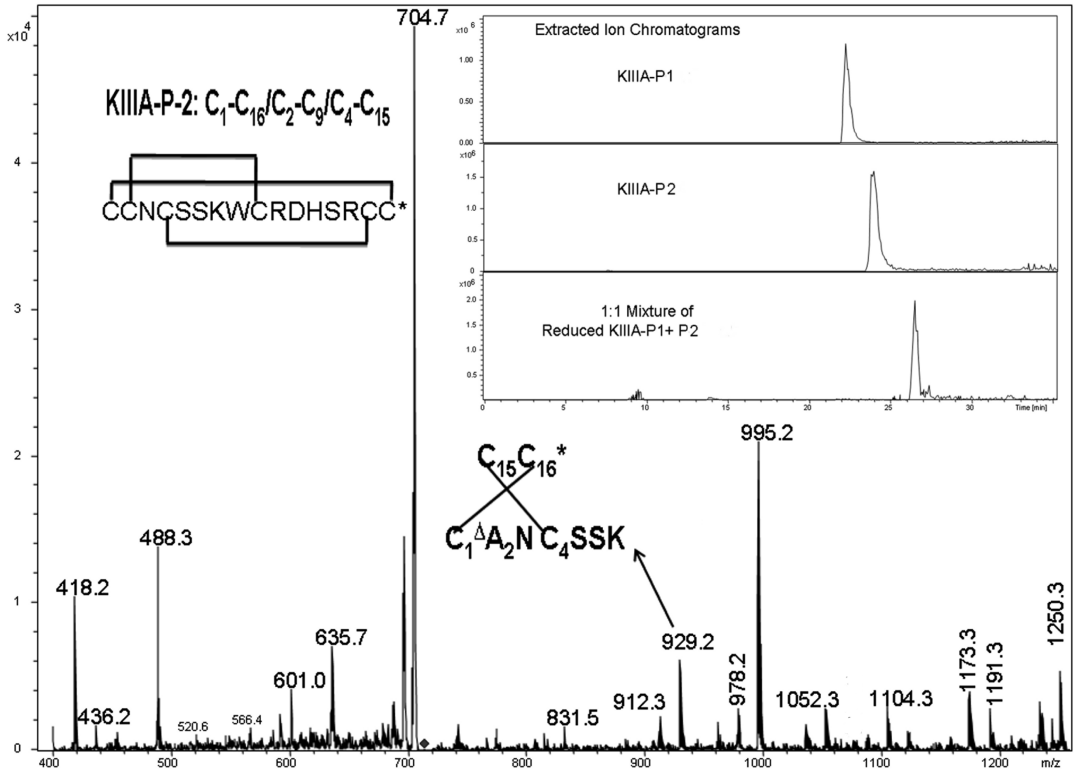

Figure 4. CID MS^2 spectrum of the peptide derived upon trypsin digestion of μ-KIIIA-P2 [m/z 712.8, $(M + 2H)^{2+}$]. The inset shows the extracted ion chromatogram from the LC−MS analysis of μ-KIIIA-P1, μ-KIIIA-P2, and a reduced equimolar mixture of both fractions.

Table 1. Structural Statistics for μ-KIIIA[C1−C15,C2−C9,C4−C16] and μ-KIIIA[C1−C9,C2−C15,C4−C16]

	μ-KIIIA[C1−C15,C2−C9,C4−C16]	μ-KIIIA[C1−C9,C2−C15,C4−C16][e]
no. of distance restraints	231	225
intraresidue ($i = j$)	97	97
sequential ($\|i - j\| = 1$)	70	70
short-range ($1 < \|i - j\| < 6$)	45	45
long-range	19	13
no. of dihedral restraints	8	8
energy E_{NOE} (kcal mol^{-1})[a]	1.7 ± 0.4	1.6 ± 0.3
deviations from ideal geometry[b]		
bonds (Å)	0.0015 ± 0.0001	0.0017 ± 0.0002
angles (deg)	0.503 ± 0.005	0.503 ± 0.013
impropers (deg)	0.379 ± 0.009	0.371 ± 0.009
mean global rmsd (Å)[c]		
backbone heavy atoms	0.51 ± 0.12	0.58 ± 0.11
all heavy atoms	1.39 ± 0.26	1.42 ± 0.28
Ramachandran plot[d] (%)		
most favored	81.1	78.9
allowed	18.9	21.1
additionally allowed	0	0
disallowed	0	0

[a]The values for E_{NOE} are calculated from a square well potential with force constants of 50 kcal mol^{-1} $Å^{-2}$. [b]The values for the bonds, angles, and impropers show the deviations from ideal values based on perfect stereochemistry. [c]The pairwise rmsd over the indicated residues calculated with MOLMOL. [d]As determined by PROCHECK-NMR for all residues except Gly and Pro. [e]Structural statistics for μ-KIIIA[C1−C9,C2−C15,C4−C16] from previously published data[22] for comparison.

structures of the fragment ions at m/z 995.2 are shown in Figure 3. The ions at m/z 656.1 and 791.2, establish the C4−C16 connectivity unambiguously. The overall connectivity pattern is therefore that of foldamer F11 (1−5/2−4/3−6).

μ-KIIIA-P2. For μ-KIIIA-P2, an identical mass was obtained upon trypsin digestion. Fragmentation of the doubly charged tryptic peptide yielded an identical MS/MS spectrum (Figure 4), which again leaves F11 and F14 as the two probable foldamers (as described previously for μ-KIIIA-P1). Unfortunately, the MS^3 fragmentation of the ion at m/z 995.2 did not yield product ions with measurable intensities. However, assignment of the disulfide connectivity in μ-KIIIA-P2 to

dx.doi.org/10.1021/bi301256s | Biochemistry 2012, 51, 9826−9835

foldamer F14 may be made through an alternative approach. As described above, the observation of the ion at m/z 995.2 is only compatible with foldamers F11 and F14. μ-KIIIA-P1 has already been assigned unambiguously, through mass spectral fragmentation, as F11. HPLC analysis of μ-KIIIA-P1 and -P2 reveals two distinct retention times, suggesting that they are indeed two distinct foldamers (inset of Figure 4). Upon reduction, the linearized product from the two foldamers must be identical. This is demonstrated by HPLC coelution of reduced products of both the μ-KIIIA foldamers (inset of Figure 4). Hence, the connectivity of μ-KIIIA-P2 is that of F14 (1−6/2−4/3−5) (Figure 4).

μ-KIIIB-P1 and -P2. Peptide μ-KIIIB, as mentioned previously, differs from μ-KIIIA by addition of an N-terminal Asn-Gly pair. In a similar way, described in the Supporting Information (Figures S3−S5 and the supplementary text), the disulfide connectivities of the μ-KIIIB isomers were determined. The disulfide connectivity of the major isomer, μ-KIIIB-P2, was determined to be 1−5/2−4/3−6, while that of μ-KIIIB-P1 was determined to be 1−6/2−4/3−5.

NMR of μ-KIIIA. Comparison of one-dimensional spectra at 5 °C of μ-KIIIA-P1 with that published originally for μ-KIIIA[22] (Figure S6 of the Supporting Information) indicates that the original sample studied was identical to μ-KIIIA-P1, the major isomer obtained from oxidative folding. Spectra of μ-KIIIA-P2, on the other hand, displayed significant differences, indicating a different fold as a result of a different disulfide connectivity (Figure S6 of the Supporting Information).

Recalculated Solution Structure for μ-KIIIA-P1. The [C1−C15,C2−C9,C4−C16] disulfide connectivity was consistent with the original NOE and dihedral data set,[22] with no major violations observed during the calculations, although there was a slight increase in the NOE energy function for the final structures calculated. A summary of experimental constraints and structural statistics for μ-KIIIA with the [C1−C15,C2−C9,C4−C16] disulfide connectivity (i.e., μ-KIIIA-P1) compared with the previously calculated structure for μ-KIIIA assuming the [C1−C9,C2−C15,C4−C16] disulfide connectivity is given in Table 1. The angular order parameters for φ and ψ in the final ensemble of 20 structures for μ-KIIIA[C1−C15,C2−C9,C4−C16] were both >0.8 over all residues (Figure S8 of the Supporting Information), indicating that the backbone dihedral angles are well-defined across the family of structures. The mean pairwise rmsd over the backbone heavy atoms over all residues for the family of structures of μ-KIIIA[C1−C15,C2−C9,C4−C16] was 0.51 Å. Comparisons of the calculated families of structures as well as closest-to-average structures of μ-KIIIA[C1−C9,C2−C15,C4−C16] and μ-KIIIA-[C1−C15,C2−C9,C4−C16] are shown in Figures 5 and 6. Similar to the findings of Poppe et al.,[17] structures recalculated with the [C1−C15,C2−C9,C4−C16] disulfide connectivity had an overall topology resembling that of the previously published structure,[22] with an α-helix spanning residues 7−12 in the closest-to-average structure. The backbones generally align well with a global rmsd of 0.57 ± 0.14 Å over residues 4−16. The main difference lies in the orientation of the N-terminus, with Cys2 now pulled closer to the α-helix and Cys1 oriented toward the C-terminal tail as a result of the C2−C9 and C1−C15 disulfide bonds, respectively. With the [C1−C15,C2−C9,C4−C16] disulfide connectivity, backbone φ and ψ angles of Cys2 correspond to the β-sheet region of the Ramachandran plot instead of the α-helix region, as observed

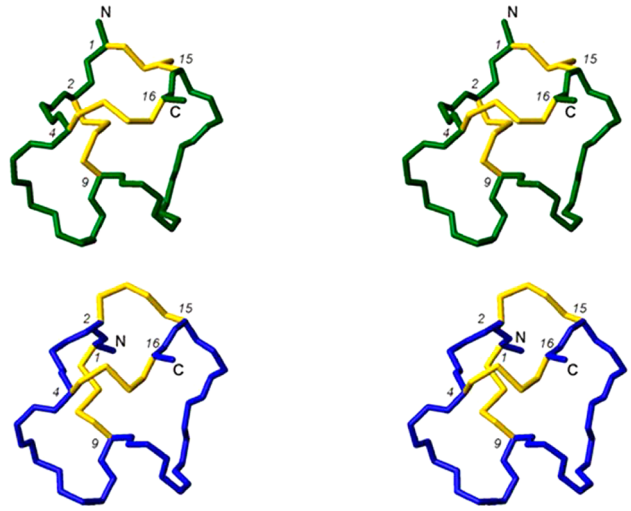

Figure 5. Stereoviews of backbone and closest-to-average structures of μ-KIIIA[C1−C15,C2−C9,C4−C16] (green) and μ-KIIIA[C1−C9,C2−C15,C4−C16][22] (blue). Disulfide bonds are colored yellow.

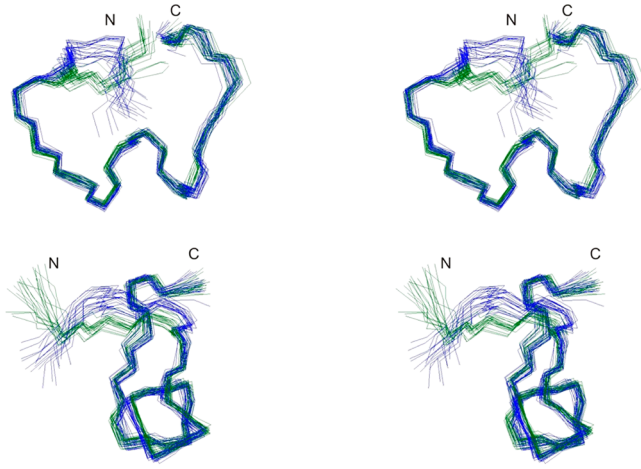

Figure 6. Stereoviews of the overlay of the ensemble of 20 NMR structures of μ-KIIIA[C1−C15,C2−C9,C4−C16] (green) and μ-KIIIA[C1−C9,C2−C15,C4−C16][22] (blue), superimposed over backbone heavy atoms of residues 4−16. Top and bottom panels are related by a 90° anticlockwise rotation about the vertical axis.

with the [C1−C9,C2−C15,C4−C16] disulfide connectivity (Figure S9 of the Supporting Information).

Electrophysiology Assays. The ability of the minor oxidative folding isomer of μ-KIIIA (μ-KIIIA-P2) and the two major oxidative folding isomers of μ-KIIIB (μ-KIIIB-P1 and μ-KIIIB-P2) to block $Na_V1.2$ expressed in oocytes was assessed by the voltage clamp protocol described in Materials and Methods. Table 2 summarizes the activity of 10 μM μ-KIIIA-P2, μ-KIIIB-P1, and μ-KIIIB-P2 on $Na_V1.2$ in comparison with that of the major oxidative folding isomer of μ-KIIIA (μ-KIIIA-P1) reported previously.[37] Representative sodium−current traces of the block by μ-KIIIB-P1 and μ-KIIIB-P2 of $Na_V1.2$ are shown in Figure S10 of the Supporting Information. Both μ-KIIIB isomers had slow off rates comparable to that of μ-KIIIA, indicating their almost irreversible binding to the $Na_V1.2$ channel. Of the two μ-KIIIB isomers, the major oxidative folding isomer, μ-KIIIB-P2, displayed a greater affinity (K_d = 0.026 μM) for $Na_V1.2$ than μ-KIIIB-P1 (K_d = 0.47 μM). Thus, μ-KIIIB-P2 was ∼5 times less potent than μ-KIIIA-P1 (K_d =

dx.doi.org/10.1021/bi301256s | *Biochemistry* 2012, 51, 9826−9835

Table 2. Block of $Na_V1.2$ by μ-KIIIA and μ-KIIIB[a]

toxin	k_{off} (min^{-1})	k_{on} (μM^{-1} min^{-1})	K_d[b] (μM)
μ-KIIIA-P1[c]	0.0016 ± 0.0016	0.30 ± 0.03	0.005 ± 0.005
μ-KIIIA-P2	0.0044 ± 0.0023	0.019 ± 0.002[d]	0.23 ± 0.12
μ-KIIIB-P1	0.0052 ± 0.0017	0.011 ± 0.003[d]	0.47 ± 0.20
μ-KIIIB-P2	0.0034 ± 0.0018	0.13 ± 0.01[d]	0.026 ± 0.014

[a]Values (mean ± standard deviation; $n \geq 3$ oocytes) were obtained by two-electrode voltage clamp of *Xenopus* oocytes expressing rat $Na_V1.2$ channels as described in Methods and Materials. [b]From k_{off}/k_{on}. [c]Values for μ-KIIIA as determined previously.[22] [d]From $(k_{obs} - k_{off})/10$ μM.

0.005 μM). Via comparison of the two μ-KIIIA isomers, the major oxidative folding isomer, μ-KIIIA-P1, was more potent than the minor isomer μ-KIIIA-P2, which had a K_d of 0.23 μM.

The minor isomer μ-KIIIA-P2 was also tested against the $Na_V1.4$ and $Na_V1.7$ subtypes, displaying K_d values of 0.83 and 1.57 μM, respectively (Table S4 of the Supporting Information). Among these three subtypes, therefore, the selectivity profile of μ-KIIIA-P2 remained the same as for the major μ-KIIIA isomer: $Na_V1.2 > Na_V1.4 > Na_V1.7$.[39]

DISCUSSION

μ-Conotoxins belonging to the M-superfamily of conotoxins have the characteristic Cys framework (−CC−C−C−CC−) of this superfamily[40] and have been subdivided previously into five branches (M1−M5) based on the number of residues between the fourth and fifth half-cystine residues. Interestingly, among known structures, different disulfide patterns can be found in the M1 (1−5/2−4/3−6), M2 (1−6/2−4/3−5), and M4 (1−4/2−5/3−6) branch conotoxins, suggesting that the number of residues in the last cysteine loop might determine the disulfide connectivity in this family.[41,42] The first class of μ-conotoxins to be characterized (sequences in Table S1 of the Supporting Information) belonged to the M4 branch, which included μ-GIIIA, μ-GIIIB, μ-PIIIA, and μ-TIIIA, and the first of these to be characterized was μ-GIIIA from *Conus geographus*.[43] Typically, early characterization involved isolation and sequencing of the venom-derived peptide,[43] following which the peptide was synthesized chemically with the disulfide bonds formed by oxidative−reductive folding with glutathione.[44] HPLC coelution with the venom-derived toxin was then employed to confirm that the synthetic peptide had a fold identical to that of the native peptide and therefore possessed the same disulfide connectivity.[23,44] Mass spectrometric methods have also been employed to elucidate disulfide connectivities.[14,26,45] Disulfide mapping was previously conducted on synthetic μ-GIIIA, establishing the disulfide pattern as 1−4/2−5/3−6.[45] Disulfide mapping with other M4 branch μ-conotoxins μ-PIIIA and μ-SxIIIA also showed that the disulfide connectivity for this class of μ-conotoxins was consistent with that of μ-GIIIA.[21,26]

Specific disulfide mapping for the newer class of μ-conotoxins belonging to the M5 branch, which includes μ-KIIIA (Table S1 of the Supporting Information), has, however, never been conducted. Disulfide connectivities were instead based on sequence alignment with the closely related μ-conotoxins in the M4 branch. Solution structures of μ-SmIIIA,[24] μ-SIIIA,[27] μ-KIIIA,[22] and most recently μ-CnIIIC[46] were determined assuming those canonical disulfide connectivities. The results of our study on μ-KIIIA now confirm that the thermodynamically favored product of oxidative folding in vitro has a disulfide connectivity pattern differing from the canonical pattern established for the M4 μ-conotoxins. The 1−5/2−4/3−6 disulfide connectivity pattern[17] adopted by the major folding isomer, μ-KIIIA-P1, is similar to that observed in the M1 branch of conotoxins, while the 1−6/2−4/3−5 pattern of the minor isomer, μ-KIIIA-P2, is similar to that of the M2 branch. Similar studies of the other M5 μ-conotoxins will need to be conducted to determine whether all conotoxins in this class also adopt the 1−5/2−4/3−6 disulfide pattern, although we note that μ-KIIIA and μ-KIIIB have a shorter first loop compared with other M5 μ-conotoxins, with only one amino acid residue between the second and third cysteine residues (Table S1 of the Supporting Information), and this may also influence folding.

In addition to the two major disulfide isomers characterized in this paper, the biological activity and structure of the disulfide-deficient analogue μ-KIIIA[C1A,C9A], which has the [C2−C15,C4−C16] disulfide connectivity, were characterized previously.[22] Intercysteine NOEs for μ-KIIIA[C1A,C9A][22] (Table S3 of the Supporting Information) were better resolved as only two disulfide bonds were present and confirmed the expected disulfide connectivity of μ-KIIIA[C1A,C9A]. It is intriguing that μ-KIIIA[C1A,C9A] showed potent blockade of $Na_V1.2$ (K_d of 8 nM, comparable to the value of 5 nM for μ-KIIIA) and $Na_V1.4$ (240 nM compared with 50 nM)[22] even though it contained C2−C15 and C4−C16 disulfides rather than the C2−C9 and C4−C16 disulfides in the major product of in vitro folding of μ-KIIIA. Clearly, several distinct disulfide connectivities are compatible with a μ-KIIIA structure capable of potent sodium channel blockade.

The biological activities and structures of the major isomers of synthetic μ-PIIIA, an M4 branch μ-conotoxin, formed during oxidative folding were investigated recently.[47] Disulfide connectivity analysis by a combination of inter-cysteine NOE analysis and MALDI-ToF MS/MS revealed different disulfide connectivities for each of the three isomers investigated, with one adopting the canonical 1−4/2−5/3−6 connectivity. Consistent with our findings for μ-KIIIA, all three disulfide isomers of μ-PIIIA were able to block $Na_V1.4$ with considerable potency.[47] In contrast to μ-KIIIA, however, the different isomers adopted different overall folds, although the two most potent isomers did retain a common helical region between Phe7 and Arg12. Intriguingly, the disulfide isomer with a 1−5/2−6/3−4 connectivity was more than twice as potent as the 1−4/2−5/3−6 disulfide isomer,[47] which is the major form of this peptide in the venom gland.[26]

These studies, together with the results presented here, highlight the different disulfide connectivities that can arise as a result of in vitro oxidative folding. The question this then poses is whether the disulfide connectivity in the major product of in vitro oxidative folding corresponds to the native disulfide pattern in the venom of the cone shell *C. kinoshitai*. Indeed, the mechanisms of oxidative folding in vivo that lead to the formation of the native toxin in the venom are still not well understood. In the biosynthesis of a conotoxin within the venom gland, several factors such as the propeptide precursor sequence, folding enzymes (protein disulfide isomerases), and molecular chaperones can play a role in directing folding and disulfide formation, allowing the efficient synthesis of the native disulfide pattern.[48] Recent work by Safavi-Hemami et al.[49] provided evidence of the presence of both the globular and ribbon forms of α-conotoxin ImI in the venom of *Conus imperialis*. Non-native disulfide isomers have also been reported

for other α-conotoxins such as α-GI and α-AuIB.[50,51] In these α-conotoxins, two additional non-native disulfide bond isomers could be formed during oxidative folding, the "ribbon" isomer (1−4/2−3 disulfide connectivity) and the "bead" isomer (1−2/3−4). Each of these two isomers adopted a fold different from that of the native isomer (1−3/2−4), which had a globular fold. Pharmacological studies have traditionally focused on the activities of the globular form, assuming this form to be the native disulfide connectivity. However, in numerous cases (e.g., α-AuIB), it is actually the ribbon form that exhibits the greatest affinity and/or potency for the molecular target.[50] Taken together, these results suggest that multiple isoforms may have evolved, yielding even greater toxin diversity within *Conus* venoms. Although these studies emphasized the presence of multiple folding isoforms of α-conotoxins, it is conceivable that multiple "misfolded" isomers of μ-conotoxins are also present in the venom and should be explored for their biological activities.

In this study, we have also addressed the ambiguity regarding the mature peptide sequence of μ-KIIIA that was derived from the cDNA clone.[31] Similar to μ-SmIIIA,[38] two putative proteolytic processing sites were identified, and to date, the shorter sequence lacking the Asn and Gly residues at the N-terminus has been taken to be the mature peptide sequence of μ-KIIIA. However, upon further examination of the cDNA sequence of μ-KIIIA, it was determined that, if cleavage occurs immediately after the putative "KR" proteolytic site in the propeptide sequence, as observed in several other μ-conotoxins (Table S2 of the Supporting Information), then the mature peptide sequence of μ-KIIIA produced in the venoms of *C. kinoshitai* would include the two additional residues preceding the N-terminus. The N-terminally extended isomer has been named μ-KIIIB, and its major folding isomer, μ-KIIIB-P2, has been shown to block $Na_V1.2$ with a K_d 5-fold greater than that of μ-KIIIA.

Our study shows that, for μ-KIIIA, both the [C1−C9,C2−C15,C4−C16] and [C1−C15,C2−C9,C4−C16] disulfide connectivities were consistent with the NMR data set, and interchanging between the two patterns altered the structure minimally, with the α-helix bearing the key residues for sodium channel blockade being preserved. This observation validates efforts to miniaturize μ-KIIIA[29] and mimic the pharmacophore in truncated, lactam-stabilized analogues of μ-KIIIA.[52] Indeed, the uncertainty surrounding disulfide bond connectivities in synthetic conotoxins provides a compelling rationale for replacing them with more stable isosteres or removing them completely with the aim of designing more stable compounds for therapeutic use.

■ ASSOCIATED CONTENT

Supporting Information

Ten figures and four tables. This material is available free of charge via the Internet at http://pubs.acs.org.

Accession Codes

Chemical shift assignments and the family of structures for μ-KIIIA-P1 have been deposited in the BioMagResBank and Protein Data Bank as entries 20048 and 2LXG, respectively.

■ AUTHOR INFORMATION

Corresponding Author

*E-mail: ray.norton@monash.edu. Telephone: (+61 3) 9903 9167. Fax: (+61 3) 9903 9582.

Funding

This work was supported in part by grants to R.S.N., G.B. and B.M.O. from the Australian Research Council (DP1094212) and National Institutes of Health Grant GM 48677 to G.B., B.M.O., and D.Y. K.G. acknowledges CSIR, Government of India, for a senior research fellowship. The work at Bangalore was supported by grants from Department of Biotechnology, Government of India. R.S.N. acknowledges fellowship support from the National Health and Medical Research Council of Australia.

Notes

The authors declare no competing financial interest.

■ ACKNOWLEDGMENTS

We thank Prof. Alan A. Goldin (University of California, Irvine,CA) for the $Na_V1.2$ and 1.4 clones, Prof. Gail Mandel (Howard Hughes Medical Institute, Portland, OR) for the $Na_V1.7$ clone, and Dr. Layla Azam (University of Utah) for preparing cRNA from these clones. We also thank Joanna Gajewiak and Konkallu H. Gowd for helpful discussions and suggestions.

■ ABBREVIATIONS

CID, collision-induced dissociation; μ-GIIIA and μ-GIIIB, μ-conotoxins GIIIA and GIIIB, respectively, from *C. geographus*; μ-KIIIA and μ-KIIIB, μ-conotoxins KIIIA and KIIIB, respectively, from *C. kinoshitai*; μ-KIIIA[C1A,C9A], μ-KIIIA with Cys1 and Cys9 replaced with Ala; MTBE, methyl *tert*-butyl ether; $Na_V1.2$, α-subunit of voltage-gated sodium channel subtype 1.2; μ-PIIIA, μ-conotoxin PIIIA from *Conus purpurascens*; μ-SIIIA, μ-conotoxin SIIIA from *Conus striatus*; μ-SmIIIA, μ-conotoxin SmIIIA from *Conus stercusmuscarum*; rmsd, root-mean-square deviation.

■ REFERENCES

(1) Khoo, K. K., and Norton, R. S. (2012) Role of disulfide bonds in peptide and protein conformation. In *Amino Acids, Peptides and Proteins in Organic Chemistry* (Hughes, A. B., Ed.) pp 395−417, Wiley-VCH, Weinheim, Germany.

(2) Trivedi, M. V., Laurence, J. S., and Siahaan, T. J. (2009) The role of thiols and disulfides on protein stability. *Curr. Protein Pept. Sci. 10*, 614−625.

(3) Gilbert, H. F. (1995) Thiol/disulfide exchange equilibria and disulfide bond stability. *Methods Enzymol. 251*, 8−28.

(4) Holmgren, A., and Bjornstedt, M. (1995) Thioredoxin and thioredoxin reductase. *Methods Enzymol. 252*, 199−208.

(5) Buczek, O., Green, B. R., and Bulaj, G. (2007) Albumin is a redox-active crowding agent that promotes oxidative folding of cysteine-rich peptides. *Biopolymers 88*, 8−19.

(6) Armishaw, C. J., Daly, N. L., Nevin, S. T., Adams, D. J., Craik, D. J., and Alewood, P. F. (2006) α-Selenoconotoxins, a new class of potent α7 neuronal nicotinic receptor antagonists. *J. Biol. Chem. 281*, 14136−14143.

(7) Walewska, A., Zhang, M. M., Skalicky, J. J., Yoshikami, D., Olivera, B. M., and Bulaj, G. (2009) Integrated oxidative folding of cysteine/selenocysteine containing peptides: Improving chemical synthesis of conotoxins. *Angew. Chem., Int. Ed. 48*, 2221−2224.

(8) Paul, M., and Donk, W. A. v. d. (2005) Chemical and enzymatic synthesis of lanthionines. *Mini-Rev. Org. Chem. 2*, 23−37.

(9) Knerr, P. J., Tzekou, A., Ricklin, D., Qu, H., Chen, H., van der Donk, W. A., and Lambris, J. D. (2011) Synthesis and activity of thioether-containing analogues of the complement inhibitor compstatin. *ACS Chem. Biol. 6*, 753−760.

(10) Muttenthaler, M., Andersson, A., de Araujo, A. D., Dekan, Z., Lewis, R. J., and Alewood, P. F. (2010) Modulating oxytocin activity

and plasma stability by disulfide bond engineering. *J. Med. Chem. 53*, 8585−8596.
(11) Platt, R. J., Han, T. S., Green, B. R., Smith, M. D., Skalicky, J., Gruszczynski, P., White, H. S., Olivera, B., Bulaj, G., and Gajewiak, J. (2012) Stapling mimics noncovalent interactions of γ-carboxyglutamates in conantokins, Peptidic antagonists of N-methyl-D-aspartic acid receptors. *J. Biol. Chem. 287*, 20727−20736.
(12) MacRaild, C. A., Illesinghe, J., van Lierop, B. J., Townsend, A. L., Chebib, M., Livett, B. G., Robinson, A. J., and Norton, R. S. (2009) Structure and activity of (2,8)-dicarba-(3,12)-cystino α-ImI, an α-conotoxin containing a nonreducible cystine analogue. *J. Med. Chem. 52*, 755−762.
(13) Robinson, A. J., van Lierop, B. J., Garland, R. D., Teoh, E., Elaridi, J., Illesinghe, J. P., and Jackson, W. R. (2009) Regioselective formation of interlocked dicarba bridges in naturally occurring cyclic peptide toxins using olefin metathesis. *Chem. Commun.*, 4293−4295.
(14) Gray, W. R. (1993) Disulfide structures of highly bridged peptides: A new strategy for analysis. *Protein Sci. 2*, 1732−1748.
(15) Gupta, K., Kumar, M., and Balaram, P. (2010) Disulfide bond assignments by mass spectrometry of native natural peptides: Cysteine pairing in disulfide bonded conotoxins. *Anal. Chem. 82*, 8313−8319.
(16) Ye, M., Khoo, K. K., Xu, S., Zhou, M., Boonyalai, N., Perugini, M. A., Shao, X., Chi, C., Galea, C. A., Wang, C., and Norton, R. S. (2012) A helical conotoxin from *Conus imperialis* has a novel cysteine framework and defines a new superfamily. *J. Biol. Chem. 287*, 14973−14983.
(17) Poppe, L., Hui, J. O., Ligutti, J., Murray, J. K., and Schnier, P. D. (2012) PADLOC: A powerful tool to assign disulfide bond connectivities in peptides and proteins by NMR spectroscopy. *Anal. Chem. 84*, 262−266.
(18) Jordan, J. B., Poppe, L., Haniu, M., Arvedson, T., Syed, R., Li, V., Kohno, H., Kim, H., Schnier, P. D., Harvey, T. S., Miranda, L. P., Cheetham, J., and Sasu, B. J. (2009) Hepcidin revisited, disulfide connectivity, dynamics, and structure. *J. Biol. Chem. 284*, 24155−24167.
(19) Lauth, X., Babon, J. J., Stannard, J. A., Singh, S., Nizet, V., Carlberg, J. M., Ostland, V. E., Pennington, M. W., Norton, R. S., and Westerman, M. E. (2005) Bass hepcidin synthesis, solution structure, antimicrobial activities and synergism, and *in vivo* hepatic response to bacterial infections. *J. Biol. Chem. 280*, 9272−9282.
(20) Mobli, M., and King, G. F. (2010) NMR methods for determining disulfide-bond connectivities. *Toxicon 56*, 849−854.
(21) Walewska, A., Skalicky, J. J., Davis, D. R., Zhang, M. M., Lopez-Vera, E., Watkins, M., Han, T. S., Yoshikami, D., Olivera, B. M., and Bulaj, G. (2008) NMR-based mapping of disulfide bridges in cysteine-rich peptides: Application to the μ-conotoxin SxIIIA. *J. Am. Chem. Soc. 130*, 14280−14286.
(22) Khoo, K. K., Feng, Z. P., Smith, B. J., Zhang, M. M., Yoshikami, D., Olivera, B. M., Bulaj, G., and Norton, R. S. (2009) Structure of the analgesic μ-conotoxin KIIIA and effects on the structure and function of disulfide deletion. *Biochemistry 48*, 1210−1219.
(23) Hill, J. M., Alewood, P. F., and Craik, D. J. (1996) Three-dimensional solution structure of μ-conotoxin GIIIB, a specific blocker of skeletal muscle sodium channels. *Biochemistry 35*, 8824−8835.
(24) Keizer, D. W., West, P. J., Lee, E. F., Yoshikami, D., Olivera, B. M., Bulaj, G., and Norton, R. S. (2003) Structural basis for tetrodotoxin-resistant sodium channel binding by μ-conotoxin SmIIIA. *J. Biol. Chem. 278*, 46805−46813.
(25) Lancelin, J. M., Kohda, D., Tate, S., Yanagawa, Y., Abe, T., Satake, M., and Inagaki, F. (1991) Tertiary structure of conotoxin GIIIA in aqueous solution. *Biochemistry 30*, 6908−6916.
(26) Shon, K. J., Olivera, B. M., Watkins, M., Jacobsen, R. B., Gray, W. R., Floresca, C. Z., Cruz, L. J., Hillyard, D. R., Brink, A., Terlau, H., and Yoshikami, D. (1998) μ-Conotoxin PIIIA, a new peptide for discriminating among tetrodotoxin-sensitive Na channel subtypes. *J. Neurosci. 18*, 4473−4481.
(27) Yao, S., Zhang, M. M., Yoshikami, D., Azam, L., Olivera, B. M., Bulaj, G., and Norton, R. S. (2008) Structure, dynamics, and selectivity of the sodium channel blocker μ-conotoxin SIIIA. *Biochemistry 47*, 10940−10949.
(28) Han, T. S., Zhang, M. M., Walewska, A., Gruszczynski, P., Robertson, C. R., Cheatham, T. E., III, Yoshikami, D., Olivera, B. M., and Bulaj, G. (2009) Structurally minimized μ-conotoxin analogues as sodium channel blockers: Implications for designing conopeptide-based therapeutics. *ChemMedChem 4*, 406−414.
(29) Stevens, M., Peigneur, S., Dyubankova, N., Lescrinier, E., Herdewijn, P., and Tytgat, J. (2012) Design of bioactive peptides from naturally occurring μ-conotoxin structures. *J. Biol. Chem. 287*, 31382−31392.
(30) Bhattacharyya, M., Gupta, K., Gowd, K. H., and Balaram, P. (2012) Rapid mass spectrometric determination of disulfide folds in peptides and proteins: A robust solution for a long standing problem in protein chemistry. *Mol. Biosyst.*, submitted.
(31) Bulaj, G., West, P. J., Garrett, J. E., Watkins, M., Zhang, M. M., Norton, R. S., Smith, B. J., Yoshikami, D., and Olivera, B. M. (2005) Novel conotoxins from *Conus striatus* and *Conus kinoshitai* selectively block TTX-resistant sodium channels. *Biochemistry 44*, 7259−7265.
(32) Biggs, J. S., Watkins, M., Puillandre, N., Ownby, J. P., Lopez-Vera, E., Christensen, S., Moreno, K. J., Bernaldez, J., Licea-Navarro, A., Corneli, P. S., and Olivera, B. M. (2010) Evolution of *Conus* peptide toxins: Analysis of *Conus californicus* Reeve, 1844. *Mol. Phylogenet. Evol. 56*, 1−12.
(33) Bartels, C., Xia, T. H., Billeter, M., Güntert, P., and Wüthrich, K. (1995) The program XEASY for computer-supported NMR spectral-analysis of biological macromolecules. *J. Biomol. NMR 6*, 1−10.
(34) Schwieters, C. D., Kuszewski, J. J., Tjandra, N., and Clore, G. M. (2003) The Xplor-NIH NMR molecular structure determination package. *J. Magn. Reson. 160*, 65−73.
(35) Laskowski, R. A., Rullmannn, J. A., MacArthur, M. W., Kaptein, R., and Thornton, J. M. (1996) AQUA and PROCHECK-NMR: Programs for checking the quality of protein structures solved by NMR. *J. Biomol. NMR 8*, 477−486.
(36) Koradi, R., Billeter, M., and Wüthrich, K. (1996) MOLMOL: A program for display and analysis of macromolecular structures. *J. Mol. Graphics 14*, 51−55 , 29−32.
(37) Zhang, M. M., Green, B. R., Catlin, P., Fiedler, B., Azam, L., Chadwick, A., Terlau, H., McArthur, J. R., French, R. J., Gulyas, J., Rivier, J. E., Smith, B. J., Norton, R. S., Olivera, B. M., Yoshikami, D., and Bulaj, G. (2007) Structure/function characterization of μ-conotoxin KIIIA, an analgesic, nearly irreversible blocker of mammalian neuronal sodium channels. *J. Biol. Chem. 282*, 30699−30706.
(38) West, P. J., Bulaj, G., Garrett, J. E., Olivera, B. M., and Yoshikami, D. (2002) μ-Conotoxin SmIIIA, a potent inhibitor of tetrodotoxin-resistant sodium channels in amphibian sympathetic and sensory neurons. *Biochemistry 41*, 15388−15393.
(39) Wilson, M. J., Yoshikami, D., Azam, L., Gajewiak, J., Olivera, B. M., Bulaj, G., and Zhang, M. M. (2011) μ-Conotoxins that differentially block sodium channels $Na_V1.1$ through 1.8 identify those responsible for action potentials in sciatic nerve. *Proc. Natl. Acad. Sci. U.S.A. 108*, 10302−10307.
(40) Norton, R. S. (2010) μ-Conotoxins as leads in the development of new analgesics. *Molecules 15*, 2825−2844.
(41) Corpuz, G. P., Jacobsen, R. B., Jimenez, E. C., Watkins, M., Walker, C., Colledge, C., Garrett, J. E., McDougal, O., Li, W., Gray, W. R., Hillyard, D. R., Rivier, J., McIntosh, J. M., Cruz, L. J., and Olivera, B. M. (2005) Definition of the M-conotoxin superfamily: Characterization of novel peptides from molluscivorous *Conus* venoms. *Biochemistry 44*, 8176−8186.
(42) Jacob, R. B., and McDougal, O. M. (2010) The M-superfamily of conotoxins: A review. *Cell. Mol. Life Sci. 67*, 17−27.
(43) Yanagawa, Y., Abe, T., Satake, M., Odani, S., Suzuki, J., and Ishikawa, K. (1988) A novel sodium channel inhibitor from *Conus geographus*: Purification, structure, and pharmacological properties. *Biochemistry 27*, 6256−6262.
(44) Cruz, L. J., Kupryszewski, G., LeCheminant, G. W., Gray, W. R., Olivera, B. M., and Rivier, J. (1989) μ-Conotoxin GIIIA, a peptide

ligand for muscle sodium channels: Chemical synthesis, radiolabeling, and receptor characterization. *Biochemistry 28*, 3437−3442.
(45) Hidaka, Y., Sato, K., Nakamura, H., Kobayashi, J., Ohizumi, Y., and Shimonishi, Y. (1990) Disulfide pairings in geographutoxin I, a peptide neurotoxin from *Conus geographus*. *FEBS Lett. 264*, 29−32.
(46) Favreau, P., Benoit, E., Hocking, H. G., Carlier, L., D'hoedt, D., Leipold, E., Markgraf, R., Schlumberger, S., Córdova, M. A., Gaertner, H., Paolini-Bertrand, M., Hartley, O., Tytgat, J., Heinemann, S. H., Bertrand, D., Boelens, R., Stocklin, R., and Molgó, J. (2012) A novel μ-conopeptide, CnIIIC, exerts potent and preferential inhibition of $Na_V1.2/1.4$ channels and blocks neuronal nicotinic acetylcholine receptors. *Br. J. Pharmacol. 166*, 1654−1668.
(47) Tietze, A. A., Tietze, D., Ohlenschlager, O., Leipold, E., Ullrich, F., Kuhl, T., Mischo, A., Buntkowsky, G., Gorlach, M., Heinemann, S. H., and Imhof, D. (2012) Structurally diverse μ-conotoxin PIIIA isomers block sodium channel $Na_V1.4$. *Angew. Chem., Int. Ed. 51*, 4058−4061.
(48) Bulaj, G., and Olivera, B. M. (2008) Folding of conotoxins: Formation of the native disulfide bridges during chemical synthesis and biosynthesis of *Conus* peptides. *Antioxid. Redox Signaling 10*, 141−155.
(49) Safavi-Hemami, H., Gorasia, D. G., Steiner, A. M., Williamson, N. A., Karas, J. A., Gajewiak, J., Olivera, B. M., Bulaj, G., and Purcell, A. W. (2012) Modulation of conotoxin structure and function is achieved through a multienzyme complex in the venom glands of cone snails. *J. Biol. Chem. 287*, 34288−34303.
(50) Dutton, J. L., Bansal, P. S., Hogg, R. C., Adams, D. J., Alewood, P. F., and Craik, D. J. (2002) A new level of conotoxin diversity, a non-native disulfide bond connectivity in α-conotoxin AuIB reduces structural definition but increases biological activity. *J. Biol. Chem. 277*, 48849−48857.
(51) Gehrmann, J., Alewood, P. F., and Craik, D. J. (1998) Structure determination of the three disulfide bond isomers of α-conotoxin GI: A model for the role of disulfide bonds in structural stability. *J. Mol. Biol. 278*, 401−415.
(52) Khoo, K. K., Wilson, M. J., Smith, B. J., Zhang, M. M., Gulyas, J., Yoshikami, D., Rivier, J. E., Bulaj, G., and Norton, R. S. (2011) Lactam-stabilized helical analogues of the analgesic μ-conotoxin KIIIA. *J. Med. Chem. 54*, 7558−7566.
(53) DeLano, W. L. (2002) *The PyMOL Molecular Graphics System*, DeLano Scientific, San Carlos, CA.